How to cite: *Angew. Chem. Int. Ed.* **2021**, *60*, 13144–13149
International Edition: doi.org/10.1002/anie.202102679
German Edition: doi.org/10.1002/ange.202102679

Computational Chemistry

Comment on "The Nature of Chalcogen-Bonding-Type Tellurium–Nitrogen Interactions": Fixing the Description of Finite-Temperature Effects Restores the Agreement Between Experiment and Theory

Jan-Michael Mewes, Andreas Hansen, and Stefan Grimme*

finite-temperature effects · gas phase · molecular dynamics · non-covalent interactions · tellurium

Abstract: *Mitzel and co-workers recently presented an intriguing molecule displaying a tellurium–nitrogen interaction. Structural data obtained in the solid and in gas phase indicated a large increase of the Te–N equilibrium distance r_e from 2.64 to 2.92 Å, respectively. Although some DFT calculations appear to support the large r_e in gas phase, we argue that the lions share of the increase is due to an incomplete description of finite-temperature effects in the back-corrected experimental data. This hypothesis is based on high-level coupled-cluster (CC) and periodic DFT calculations, which consistently point towards a much smaller r_e in the isolated molecule. Further support comes through MD simulations with a tuned GFN2-xTB Hamiltonian: Calibrated against a CC reference, these show a six-times larger influence of temperature than with the originally used GFN1-xTB. Taking this into account, the back-corrected r_e in gas phase becomes 2.67 ± 0.08 Å, in good agreement with high-level CC theory and most DFT methods.*

Non-covalent interactions (NCIs) are fundamental to the three dimensional structure of matter.[1–6] By developing a better understanding for them,[7–12] chemists have gained access to many new ways to shape matter, e.g., through self-assembly of large molecules in solution or pattern recognition.[6,13–19] Emerging from this line of research, several novel NCI motifs have been suggested and debated in recent years.[5,14–17] One of these candidates is the tellurium-nitrogen interaction displayed by the molecule recently presented by Mitzel and co-workers, in which a NMe_2 donor bonds to the σ-hole of a $Te(C_5F_5)$ fragment.[20] An important part in the rationalization and exploitation of such interactions in applications is to understand them through the interplay of experiment and theory, e.g., by providing experimental reference structures as benchmarks for theoretical approaches.[8,9,11,12,21–23] In this context, accurate gas-phase structures and properties of molecules with NCIs are a particularly appealing target as they can be directly compared to theory due to the absence of crystal-packing or solvent effects.[17,21–26]

However, measuring molecular properties in the gas phase prerequisites evaporation, which usually requires some heating, and herein lies the caveat: Due to the typically weak nature of NCIs, high temperature can significantly affect the effective (average) molecular structure and, in turn, the molecular properties. Taking this into account in the refinement of the experimental results, for example to back-correct the gas-phase electron-diffraction (GED) data to obtain equilibrium distances r_e, is by no means a trivial task.[27] Since the respective protocols themselves often rely heavily on theory and simulation, great care has to be taken, in particular when approximate semi-empirical methods are used for "exotic" types of interactions. In such situations, semi-empirical methods should always subjected some kind of sanity-check, which Mitzel and co-workers conducted in most related cases,[21–23] and which we deliver for their latest example here.

Let us begin the analysis by reviewing some key aspects of the methods used to obtain the structural data presented by Mitzel and co-workers.[20] Solid data was recorded using X-ray diffraction (XRD) at 100 K, such that finite-temperature (finite-T) effects are small, or in other words $r_{exp} = r_0 \approx r_e$ (neglecting zero-point vibrational effects). Gas-phase electron-diffraction (GED), however, was carried out using a molecular beam at low pressure and 444 ± 1 K, which was required to achieve evaporation. Interpretation of this data relies on PBE0-D3/def2-TZVP structures and path-integral

[*] Dr. J.-M. Mewes, Dr. A. Hansen, Prof. S. Grimme
Mulliken Center for Theoretical Chemistry, Institut für Physikalische und Theoretische Chemie, Rheinische Friedrich-Wilhelms Universität Bonn
Beringstraße 4, 53115 Bonn (Germany)
E-mail: janmewes@janmewes.de

Supporting information and the ORCID identification number(s) for the author(s) of this article can be found under: https://doi.org/10.1002/anie.202102679.

molecular-dynamics (PIMD) simulations with a semi-empirical quantum-mechanical GFN1-xTB Hamiltonian[28] (in the following just GFN1) to account for finite-T effects. Note that the protocol for the refinement provided in the original article is incomplete and the authors have in the meantime provided a corrigendum. As we will demonstrate, GFN1 provides a very poor description of the Te-N potential-energy surface (PES) along the stretching coordinate (too short r_e, much too large interaction energy), such that it severely underestimates finite-T effects. We hypothesize that as a result, the back-correction for the experimentally measured Te-N distance is too small and the reported r_e too large, leading to a subtantial deviation of about 0.15-0.25 Å from DFT and high-level coupled-cluster theory.

To corroborate this hypothesis, we first establish a reference for the shape and depth of the PES of the Te-N distance. To this end, we conducted a relaxed scan of the Te-N distance (*cf.* Figure 1) with the recently presented r^{2}SCAN-3c composite density-functional theory (DFT) method,[29,30] followed by single-point calculations with numerically converged domain-based local-pair natural-orbital (DLPNO) coupled-cluster (CC) with singles, doubles, and iterative triples substitutions at the estimated basis set limit (DLPNO-CCSD(T1)/CBS, estimated error ± 0.2 kcal mol^{-1}, see computational details).[31,32] Further calculations have been conducted with the same methods used by Mitzel and co-workers (M06-2X,[33] PBE0-D3,[34,35] and GFN1)[36] as well as with GFN2 and variants thereof.[37,38] Additional results for MP2, B3LYP-D4,[39–42] ωB97X-V[43,44] can be found in the supporting information.

Inspection of the PES displayed in Figure 1 shows that the CC reference predicts an r_e of only 2.67 Å, substantially shorter than most hybrid functionals and over 0.2 Å below the back-corrected experimental value. Already this tremendous deviation from such a robust high-level of theory should give pause for thought. Although all hybrid-DFT approaches tend to overestimate r_e, none of them comes even close to r_e derived from the GED experiment. The best agreement with the CC reference r_e is provided by r^{2}SCAN-3c, followed by PBE0-D3, while M06-2X overestimates r_e by more than 0.1 Å (also B3LYP-D4 and ωB97X-V). However, since the interaction is rather weak, small errors in the potential-energy surface (PES) can lead to a large variations in r_e. Accordingly, the interaction energy of all DFT methods at their respective r_e agrees reasonably well with the reference ($\Delta E < 1.5$ kcal mol^{-1}).

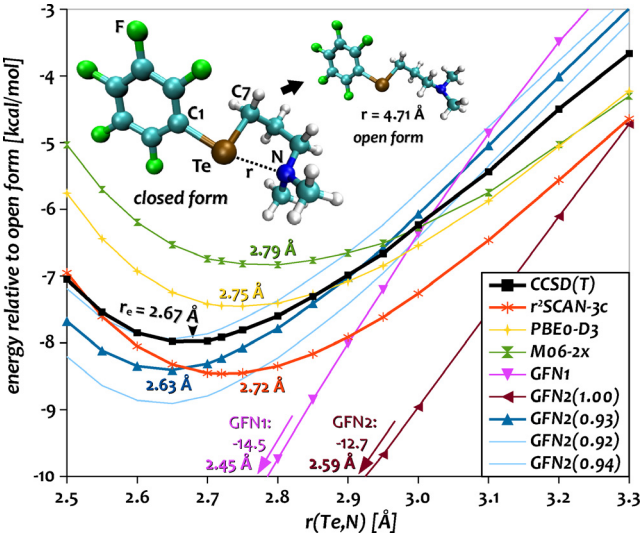

Figure 1. Scan of the potential-energy surface of the Te-N distance connecting the closed and open forms, which involves a torsion of the propyl-chain as shown in the inlay. Structures are obtained at the r^{2}SCAN-3c level, while all other methods refer to single-point calculations (see computational details). Minima calculated from a fifth-order polynomial fit are also provided. GFN2(X) refers to a modified Hamiltonian in which the zeroth-order Te-N interaction is scaled with X.

In contrast to DFT, GFN1/2 deviate more strongly, predicting a much too strong interaction and too short r_e. With GFN1, also the general shape of the PES is wrong, i.e., too attractive near r_e yet too repulsive at larger distances. Hence, in simulations with canonical GFN, the Te-N distance will remain much too close to r_e at any given temperature. However, through slight modification of the atom-pairwise GFN2 parameters, which we term H_0-tuning, the agreement with the reference can be greatly improved. For this, the zeroth-order Hamiltonian H_0 for the Te-N interaction is scaled by a factor of 0.93. The underlying idea is to restore and correct the critical relation between potential-depth (interaction strength) and available kinetic energy (temperature). A closely related approach, the so-called λ-scaling, has been employed successfully in the framework of free-energy calculations.[45–47] Here, we have chosen a scaling factor of 0.93 to balance the steeper run and thus higher energy at intermediate distances (> 2.9 Å) against the slightly deeper minimum (*cf.* blue line Figure 1). As evident from the a variation of the scaling factor by ± 0.01 (thin blue lines), it has a small linear influence on the energy of merely ± 0.5 kcal mol^{-1}.

The picture derived from the PES scan is confirmed by free optimizations of the molecule and solid, which are summarized in Table 1. For example, the Te-N distance

Table 1: Structural parameters in the solid and in gas phase from DFT, GFN variants, and from X-ray diffraction (XRD, 100 K) and gas-phase electron diffraction (GED, 445 K).[20] Distances are given in Å, angles in degree. For the atom numbers see Figure 1, the angles are α_1 = (C1,Te,N), α_2 = (C1,Te,C7). Values closest to exp. are set in **bold**.

Solid	*r*(N,Te)	*r*(C1,Te)	*r*(C7,Te)	α_1	α_2
XRD	2.639	2.189	2.159	166.4	91.3
r^{2}SCAN-3c	**2.631**	**2.217**	2.185	165.8	90.7
PBE-D	2.624	2.223	2.187	**166.4**	**90.9**
M06-L	2.731	2.220	**2.178**	167.6	93.9
Gas phase	***r*(N,Te)**	***r*(C1,Te)**	***r*(C7,Te)**	**α_1**	**α_2**
GED	2.918	2.144	2.151	161	88.6
r^{2}SCAN-3c	2.708	2.175	2.189	165.8	**91.5**
PBE0-D3	2.751	2.151	**2.158**	165.9	92.1
PBE-D4	2.757	2.175	2.186	166.3	92.2
M06-2X	2.786	2.155	2.160	**165.3**	92.1
M06-L	**2.854**	2.160	2.176	165.8	93.5
GFN2(0.93)	2.624	**2.143**	2.173	172.7	97.2
GFN2(1.00)	2.594	2.153	2.168	172.4	96.6
GFN1(1.00)	2.464	2.162	2.168	171.8	94.2

obtained by free optimization with PBE0-D3 in the isolated molecule is 2.75 Å, and thus identical to the r_e dervived from the PES scan. This is despite significant differences in the adjacent Te-C bondlengths between r^{2}SCAN-3c and PBE0-D3 (see Table 1). The value is moreover consistent with ref. [20]. In case of r^{2}SCAN-3c, the slight deviation between r_e obtained from the PES scan and free optimization (2.71 Å vs. 2.72 Å) is due to a finer integration grid used in the free optimization. With M06-2X, the free optimization provides an r_e of 2.79 Å, which is again identical to the value from the PES scan, but much smaller than the value of 2.90 Å reported by Mitzel and co-workers. This appears to be a mistake, since an M06-2x structure provided the in supporting information closely agrees with our results.[20] While exploring this issue, we noticed that the Te-N distance in the molecule is particularly sensitive to the integration grid with r^{2}SCAN-3c, M06-L, and M06-2x. Similar findings have already been reported in previous studies.[29,48,49] We thus conducted all DFT optimizations with finer grids (see SI for details).

Concerning the agreement between the molecular optimizations and the back-corrected GED structure, it appears at first glance that the Minnesota functionals M06-2x (hybrid with 54% exact exchange) and particularly M06-L (local mGGA) provide the best agreement for the Te-N distance. However, they strongly disagree with the CC reference and most other functionals. We thus think this is the result of a fortuitous error-compensation with the incomplete description of finite-T effects. This hypothesis is further substantiated by the DFT calculations for the solid with periodic boundary conditions: While both, r^{2}SCAN-3c and PBE-D4 provide remarkable agreement with the solid XRD structure and a rather short r_e in the molecule in agreement with the CC reference, M06-L predicts a too large r_e (+0.1 Å) in the solid and thus presumably also in the molecule. Note that we used the local (m)GGAs PBE-D4 and M06-L in the calculations with periodic boundary conditions instead of the respective hybrid functionals PBE0-D3 and M06-2X since the calculations with non-local Fock exchange and reasonably converged basis sets and *k*-point grids are prohibitively expensive.

In the next step, we explore the impact of finite-T effects through Born-Oppenheimer molecular-dynamics (MD) simulations, and compare how the predicted averages differ between GFN1 used in the original work, and the H_0-tuned GFN2 which provides the correct interaction strength. For this purpose, we collected a total of 0.50 µs of MD simulations with the H_0-tuned GFN2 Hamiltonian for a range of temperatures, as well as with variations of H_0-tuned GFN2 and canonical GFN1 at 445 K. For each run, we calculated the average Te-N distance $<r>$ as well as the standard deviation using block-averaging. Note that very long simulation times of 50 ns were required to properly converge the simulation averages at the elevated temperatures. These data are visualized together with a polynomial fit in Figure 2.

Inspection of the results for H_0-tuned GFN2(0.93) reveals an near-linear increase of $<r>$ from 100 K to about 350 K, followed by a sharp increase from 350 K onward. These results show that irrespective of small variations in the scaling factor, i.e, for interaction energy of $\approx$8 kcal mol^{-1}, the average Te-N distance substantially increases in the experimental temperature range, indicating a beginning dissociation. This is in stark contrast to the results obtained with canonical GFN1. Here, due to the much stronger interaction of $\approx$14.5 kcal mol^{-1}, finite temperature effects are not nearly as large at 445 K. With a Δr_e of only 0.05 Å, the shift is six times smaller than with GFN2(0.93). Accordingly, the GFN1-based back-corrections for finite-T effects applied to the GED data are certainly too small. To correct for this, we first remove the GFN1 back-correction from the GED value of Mitzel and co-workers, which provides the uncorrected experimental value of 2.97 ± 0.02 Å. From this value, we either subtract the GFN2 back-correction of 0.30 ± 0.03 Å, which provides an r_e = 2.67 ± 0.04 Å in excellent agreement with the CC reference. Alternatively, as is shown in Figure 2, we can subtract r_e calculated with the CC reference to obtain the size of finite-T effects Δr_e = 0.30 ± 0.02 Å, which agrees nicely with the result from the GFN2(0.93) simulations. Based on these considerations, we suggest an improved back-corrected gas-phase r_e of 2.67 ± 0.08 Å, where the uncertainty accounts for variation in the Te-N PES (H_0-scaling factor) and temperature.

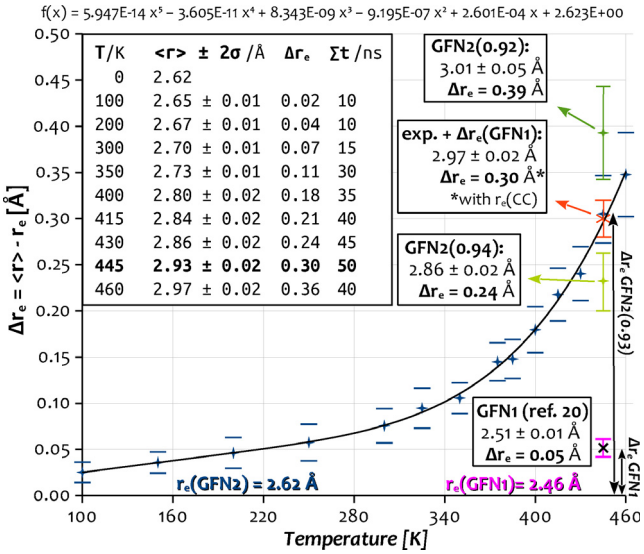

Figure 2. Increase of the Te-N distance ($<r>$-r_e) and standard deviation from the GFN2(0.93) and GFN1 MD simulations plotted against temperature. 5th order polynomial fit of the absolute GFN2(0.93) values given at the top. Data for GFN2(0.92) and (0.94) shown in green (50 ns simulation time each), GFN1 in pink, experimental data relative to the DLPNO-CCSD(T1) r_e in orange. Length of the simulation and values are provided in the inlay. Crosses show the average distance, while horizontal bars mark the 2-σ range.

The last point we want to explain is why a single conformer was apparently sufficient to achieve good agreement with the experimentally observed GED spectrum, as pointed out by Mitzel and workers.[20] For this, we inspect the radial distribution function (RDF) of the Te-N couple obtained at 300 K, 400 K, and 445 K, which is displayed in Figure 3. Evidently, there is no distinct second maximum in the RDF at 445 K. The value of the integral increases smoothly beyond the maximum of the RDF at $\Delta r_e \approx$ 0.05 Å, which is similar for all shown simulations. Our interpretation of this data is that at 445 K, about 10% of the population exist

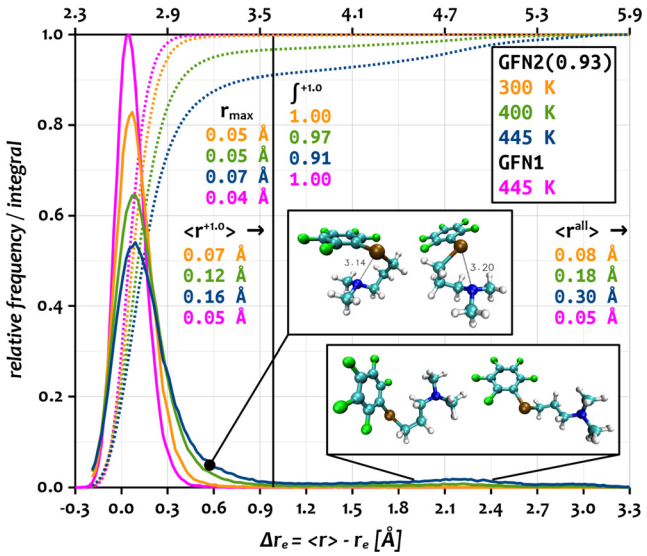

Figure 3. Frequency (solid lines, relative to GFN1) and integral (dotted lines) of the RDF of the increase of the Te-N distance for $T = 300$ K, 400 K, and 445 K with H_0-tuned GFN2 and with canonical GFN1 using 2 pm wide bins. The inlays provide the maximum increase r_{max}, the average increase for all configurations up to an increase of 1.0 Å $< r^{+1.0} >$, and the average increase for the whole range $< r^{all} >$, as well as some representative structures. The scale at the top shows the absolute $< r >$ for the GFN2(0.93) simulations.

in the open form (see inlay), i.e., without the Te-N interaction, corresponding to distance of roughly 4.8 Å. This nicely agrees with the r_e of the open form shown in Figure 1. Due to the inherent floppiness of the propyl-chain linking N and Te, the open form can not be described as a single conformer. Instead, the RDF for 445 K shows a smeared out second maximum centred at around 4.8 Å, corresponding to a plethora of conformers with a broken Te-N interaction. This large number of micro states on a shallow PES is equivalent to a large entropic stabilization, explaining why this form is significantly populated in the MD despite its high energy, for which a simple Boltzmann-Ansatz (no degeneracy) provides a population $< 1\,\%$ at 445 K for $\Delta G = 8$ kcal mol^{-1}. Accordingly, due to the inherent anharmonicity, it is very questionable if static thermochemical calculations based on the harmonic approximation can correctly describe the equilibrium between the closed and open forms, even if zero-point energies as well as enthalpic and entropic finite-temperature corrections are included.

In fact, nearly half of the increase of $< r >$ at 445 K is due to contributions from the open form and not due to the shoulder right of the main peak, which mostly consists of conformers featuring a side-on Te-N interaction. This is evident from a comparison of the averages calculated for all configurations up to an increase of 1.0 Å $< r^{+1.0} >$ (black vertical line), and the average calculated for the whole range $< r^{all} >$ for the three temperatures shown in Figure 3. As a result of the beginning dissociation in the experimental temperature range, $< r >$ is highly susceptible to small changes in the energetic difference between the open and the closed forms (*cf.* GFN2(0.92) and GFN2(0.94) with $\Delta E \approx 1$ kcal mol^{-1} shown in Figure 2 in green). Accordingly, with GFN1, which overestimates the Te-N interaction almost by a factor of two, the open form is not at all populated at 445 K, such that finite-T effects are much too small.

In summary, we have conclusively demonstrated that the large back-corrected $r_e = 2.92$ Å reported for Te-N distance in the gas phase results from an incomplete description of finite-T effects. This was traced back to an almost two-fold overestimation of the Te-N interaction energy by GFN1, which was used in the original refinement protocol. Using a H_0-tuned GFN2 Hamiltonian calibrated against numerically converged DLPNO-CCSD(T1), we observed a beginning dissociation, leading to a six-fold increase of finite-T effects on r(Te,N) at the experimental $T = 445$ K compared to GFN1. Based on these improved simulations, we suggested a back-corrected r_e of 2.67 ± 0.08 Å, restoring the agreement with high-level CC calculations and DFT.

In passing, we note that prominent hybrid functionals (M06-2X, B3LYP-D4, and ωB97X-V) significantly and systematically overestimate the Te-N equilibrium distance ($\Delta r_e > 0.1$ Å) compared to the CC reference. This is in part due to the weakness of the interaction, where small errors in the potential can exert a large influence on r_e. Accordingly, the agreement of the DFT methods for the interaction energy at r_e is more consistent: r^{2}SCAN-3c, PBE0-D3, and B3LYP-D4 are all accurate to within 0.5 kcal mol^{-1}, while the other tested functionals show only slightly larger deviations ($\Delta E \approx 1$ kcal mol^{-1}). This means that a comparison of the semi-empirical GFN1 Hamiltonian to any of the tested DFT methods would have revealed the strong over-binding. Finally, we want to point out that the recently presented composite method r^{2}SCAN-3c provides the best agreement with the CC reference (and XRD) for the (solid) structure and energy at less than one hundredth of the cost of hybrid-DFT/QZ approaches.[29]

We conclude with the suggestion to take great care when using approximate semi-empirical methods to model "exotic" non-covalent interactions, e.g., in MD simulations. In such a scenario, semi-empirical approaches should be subjected to at least basic sanity-checks and cross-validated against more robust references. As evident from the results shown here, dispersion-corrected (hybrid) DFT can often serve this purpose nearly as well if high-level CC references are prohibitively expensive. In case of a severe deviation between the reference and semi-empirical GFN1/GFN2, the presented H_0-tuning constitutes a straightforward approach to correct for the deficiencies of semi-empirical methods and to conduct even nanosecond MD simulations with reasonable computational resources.

Computational Details

All DFT, MP2, and CC results shown in Figure 1 were obtained with the ORCA 4.2.1 program package.[50,51] They employ the frozen-core and RI approximations for the post-Hartree–Fock part, TightSCF convergence criteria in the Hartree–Fock iterations and default integration grids. The domain-based pair-natural-orbital local coupled-cluster method[32] was used in its sparse-maps[52] iterative-triples[32] implementation (DLPNO-CCSD(T1)) with VeryTightP-

NO[53] threshold settings. An aug-cc-pVTZ/aug-cc-pVQZ complete basis-set (CBS) extrapolation[54] was carried out for MP2 (with matching auxiliary basis sets),[55] while the DLPNO-CCSD(T1) reference values were obtained with an additive CBS extrapolation-Scheme based on focal-point analysis.[56] The residual error of the latter is conservatively estimated at ± 0.2 kcal mol^{-1} (see the supplementary material for details). PBE0-D3 and M06-2X were evaluated in the def2-TZVP and def2-TZVPP basis sets,[57] to be consistent with the work of Mitzel and co-workers. B3LYP-D4 and ωB97X-V employ the numerically converged def2-QZVPP basis.[57] The D3 correction was applied with Becke-Johnson damping[35,58] and the D4 correction was calculated with the respective standalone program.[41,42,59]

All DFT calculations reported in Table 1 have been conducted with TURBOMOLE 7.5.1[60–64] employing default convergence and increased grid settings (gridsize m5, see the supplementary material for details). Calculations with PBE-D4 and M06-L use the def2-TZVP and def2-TZVPP basis sets, respectively. Calculations with periodic boundary conditions employ a $3\times2\times3$ *k*-point grid. The Stuttgart-Dresden def2-ECP was used for Te in all calculations.[65]

GFN2-xTB calculations and MD simulations were conducted with xTB 6.4.0.[37] MD simulations use an Anderson thermostat with a time-step of 4 fs, for which all bonds involving hydrogen are constrained. With these settings, the GFN2 MD simulations on one core of a reasonably modern CPU (Intel(R) Xeon(R) Gold 6148 @ 2.4 GHz) progress with about 300 ps (75k steps) per hour walltime. MDs have a length of 5 ns, the first 200 ps of which are considered equilibration.

For the H_0-tuning of the GFN2 Hamiltonian, the lines

```
$pairpar
7 52 value
$end
```

are added to the GFN2 parameter file. Radial-distribution functions and their integrals were evaluated using the Travis program.[66]

Supplementary Material

In the Supporting Information, we provide the structures representing the PES shown in Figure 1 (xyz files), all numerical values (data.ods), details on the calculation of the CC reference values (pdf file), the optimized molecular and solid structures given in Table 1 (xyz and coord files), an investigation of the grid dependence of the mGGA methods (M06-L, M06-2x, r^{2}SCAN-3c, pdf file), as well a spreadsheet with the data from the MDs shown in Figures 2 and 3 (data.ods).

Acknowledgements

This work was supported by the DFG in the framework of the priority program 1807 "Control of London dispersion interactions in molecular chemistry". J.-M.M. thanks S. Schmitz and M. Bursch for proofreading the manuscript. Open access funding enabled and organized by Projekt DEAL.

Conflict of interest

The authors declare no conflict of interest.

[1] J. W. Steed, J. L. Atwood, *Supramolecular chemistry*, Wiley, Hoboken, **2013**.
[2] J.-M. Lehn, *Science* **1993**, *260*, 1762 – 1764.
[3] A. O. de la Roza, G. A. DiLabio, *Non-covalent Interactions in Quantum Chemistry and Physics: Theory and Applications*, Elsevier, Amsterdam, **2017**.
[4] H.-J. Schneider, *Angew. Chem. Int. Ed.* **2009**, *48*, 3924 – 3977; *Angew. Chem.* **2009**, *121*, 3982 – 4036.
[5] A. S. Mahadevi, G. N. Sastry, *Chem. Rev.* **2013**, *113*, 2100 – 2138.
[6] K. E. Riley, P. Hobza, *Acc. Chem. Res.* **2013**, *46*, 927 – 936.
[7] C. Bleiholder, D. B. Werz, H. Köppel, R. Gleiter, *J. Am. Chem. Soc.* **2006**, *128*, 2666 – 2674.
[8] S. Grimme, A. Hansen, J. G. Brandenburg, C. Bannwarth, *Chem. Rev.* **2016**, *116*, 5105 – 5154.
[9] F. Biedermann, H.-J. Schneider, *Chem. Rev.* **2016**, *116*, 5216 – 5300.
[10] M. Bursch, E. Caldeweyher, A. Hansen, H. Neugebauer, S. Ehlert, S. Grimme, *Acc. Chem. Res.* **2019**, *52*, 258 – 266.
[11] M. Bursch, L. Kunze, A. M. Vibhute, A. Hansen, K. M. Sureshan, P. G. Jones, S. Grimme, D. B. Werz, *Chem. Eur. J.* **2021**, *27*, 4627 – 4639.
[12] N. Mehta, T. Fellowes, J. White, L. Goerigk, *chemrxiv* **2021**, https://doi.org/10.26434/chemrxiv.13521377.v1.
[13] R. Gleiter, G. Haberhauer, D. B. Werz, F. Rominger, C. Bleiholder, *Chem. Rev.* **2018**, *118*, 2010 – 2041.
[14] D. B. Werz, R. Gleiter, F. Rominger, *Organometallics* **2003**, *22*, 843 – 849.
[15] S. Saha, G. R. Desiraju, *Chem. Eur. J.* **2017**, *23*, 4936 – 4943.
[16] P. Scilabra, G. Terraneo, G. Resnati, *Acc. Chem. Res.* **2019**, *52*, 1313 – 1324.
[17] O. Dumele, B. Schreib, U. Warzok, N. Trapp, C. A. Schalley, F. Diederich, *Angew. Chem. Int. Ed.* **2017**, *56*, 1152 – 1157; *Angew. Chem.* **2017**, *129*, 1172 – 1177.
[18] A. Vanderkooy, A. K. Gupta, T. Földes, S. Lindblad, A. Orthaber, I. Pápai, M. Erdélyi, *Angew. Chem. Int. Ed.* **2019**, *58*, 9012 – 9016; *Angew. Chem.* **2019**, *131*, 9110 – 9114.
[19] Z. M. Efimenko, A. A. Eliseeva, D. M. Ivanov, B. Galmés, A. Frontera, N. A. Bokach, V. Y. Kukushkin, *Crystal Growth Design* **2021**, *21*, 588 – 596.
[20] T. Glodde, Y. V. Vishnevskiy, L. Zimmermann, H.-G. Stammler, B. Neumann, N. W. Mitzel, *Angew. Chem. Int. Ed.* **2021**, *60*, 1519 – 1523; *Angew. Chem.* **2021**, *133*, 1542 – 1546.
[21] N. W. Mitzel, U. Losehand, A. Wu, D. Cremer, D. W. H. Rankin, *J. Am. Chem. Soc.* **2000**, *122*, 4471 – 4482.
[22] N. W. Mitzel, K. Vojinovi c, R. Fröhlich, T. Foerster, H. E. Robertson, K. B. Borisenko, D. W. H. Rankin, *J. Am. Chem. Soc.* **2005**, *127*, 13705 – 13713.
[23] M. Hagemann, R. J. F. Berger, S. A. Hayes, H.-G. Stammler, N. W. Mitzel, *Chem. Eur. J.* **2008**, *14*, 11027 – 11038.
[24] A. Bhattacherjee, S. Wategaonkar, *J. Phys. Chem. A* **2017**, *121*, 8815 – 8824.
[25] R. Chaudret, B. de Courcy, J. Contreras-García, E. Gloaguen, A. Zehnacker-Rentien, M. Mons, J.-P. Piquemal, *Phys. Chem. Chem. Phys.* **2014**, *16*, 9876 – 9891.
[26] G. Pietraperzia, M. Pasquini, F. Mazzoni, G. Piani, M. Becucci, M. Biczysko, D. Michalski, J. Bloino, V. Barone, *J. Phys. Chem. A* **2011**, *115*, 9603 – 9611.
[27] Y. V. Vishnevskiy, J. Schwabedissen, A. N. Rykov, V. V. Kuznetsov, N. N. Makhova, *J. Phys. Chem. A* **2015**, *119*, 10871 – 10881.
[28] S. Grimme, C. Bannwarth, P. Shushkov, *J. Chem. Theory Comput.* **2017**, *13*, 1989 – 2009.
[29] S. Grimme, A. Hansen, S. Ehlert, J.-M. Mewes, *J. Chem. Phys.* **2021**, *154*, 064103.
[30] J. W. Furness, A. D. Kaplan, J. Ning, J. P. Perdew, J. Sun, *J. Phys. Chem. Lett.* **2020**, *11*, 8208 – 8215.

[31] C. Riplinger, B. Sandhoefer, A. Hansen, F. Neese, *J. Chem. Phys.* **2013**, *139*, 134101.
[32] Y. Guo, C. Riplinger, U. Becker, D. G. Liakos, Y. Minenkov, L. Cavallo, F. Neese, *J. Chem. Phys.* **2018**, *148*, 011101.
[33] Y. Zhao, D. G. Truhlar, *Theor. Chem. Acc.* **2008**, *120*, 215 – 241.
[34] C. Adamo, V. Barone, *J. Chem. Phys.* **1999**, *110*, 6158 – 6170.
[35] S. Grimme, S. Ehrlich, L. Goerigk, *J. Comput. Chem.* **2011**, *32*, 1456 – 1465.
[36] Semiempirical Extended Tight-Binding Program Package xtb, https://github.com/grimme-lab/xtb. Accessed: 2021-01-18.
[37] C. Bannwarth, S. Ehlert, S. Grimme, *J. Chem. Theory Comput.* **2019**, *15*, 1652 – 1671.
[38] C. Bannwarth, E. Caldeweyher, S. Ehlert, A. Hansen, P. Pracht, J. Seibert, S. Spicher, S. Grimme, *WIREs Comput. Mol. Sci.* **2020**, e01493.
[39] A. D. Becke, *Phys. Rev. A* **1988**, *38*, 3098.
[40] A. D. Becke, *J. Chem. Phys.* **1993**, *98*, 5648 – 5652.
[41] E. Caldeweyher, S. Ehlert, A. Hansen, H. Neugebauer, S. Spicher, C. Bannwarth, S. Grimme, *J. Chem. Phys.* **2019**, *150*, 154122.
[42] E. Caldeweyher, J.-M. Mewes, S. Ehlert, S. Grimme, *Phys. Chem. Chem. Phys.* **2020**, *22*, 8499 – 8512.
[43] N. Mardirossian, M. Head-Gordon, *Phys. Chem. Chem. Phys.* **2014**, *16*, 9904 – 9924.
[44] O. A. Vydrov, T. Van Voorhis, *J. Chem. Phys.* **2009**, *130*, 104105.
[45] J.-M. Mewes, O. R. Smits, G. Kresse, P. Schwerdtfeger, *Angew. Chem. Int. Ed.* **2019**, *58*, 17964 – 17968; *Angew. Chem.* **2019**, *131*, 18132 – 18136.
[46] J.-M. Mewes, O. R. Smits, *Phys. Chem. Chem. Phys.* **2020**, *22*, 24041 – 24050.
[47] J.-M. Mewes, P. Schwerdtfeger, *Angew. Chem. Int. Ed.* **2021**, *60*, 7703 – 7709; *Angew. Chem.* **2021**, *133*, 7782 – 7788.
[48] L. Goerigk, *J. Phys. Chem. Lett.* **2015**, *6*, 3891 – 3896.
[49] N. Mardirossian, M. Head-Gordon, *J. Theor. Comput. Chem.* **2013**, *9*, 4453 – 4461.
[50] F. Neese, *WIREs Comput. Mol. Sci.* **2018**, *8*, 8:e1327.
[51] F. Neese, ORCA—An Ab Initio, DFT and Semiempirical electronic structure package, Ver. 4.2.1 (Max Planck Institut für Kohlenforschung, Mülheim, Germany, 2020).
[52] C. Riplinger, P. Pinski, U. Becker, E. F. Valeev, F. Neese, *J. Chem. Phys.* **2016**, *144*, 024109.
[53] F. Pavošević, C. Peng, P. Pinski, C. Riplinger, F. Neese, E. F. Valeev, *J. Chem. Phys.* **2017**, *146*, 174108.
[54] T. Helgaker, W. Klopper, H. Koch, J. Noga, *J. Chem. Phys.* **1997**, *106*, 9639 – 9646.
[55] R. A. Kendall, T. H. Dunning, R. J. Harrison, *J. Chem. Phys.* **1992**, *96*, 6796 – 6806.
[56] A. G. Császár, W. D. Allen, H. F. Schaefer, *J. Chem. Phys.* **1998**, *108*, 9751 – 9764; M. S. Marshall, L. A. Burns, C. D. Sherrill, *J. Chem. Phys.* **2011**, *135*, 194102.
[57] F. Weigend, R. Ahlrichs, *Phys. Chem. Chem. Phys.* **2005**, *7*, 3297 – 3305.
[58] S. Grimme, J. Antony, S. Ehrlich, H. Krieg, *J. Chem. Phys.* **2010**, *132*, 154104.
[59] Generally Applicable Atomic-Charge Dependent London Dispersion Correction dftd4.“, https://github.com/dftd4/dftd4. Accessed: 2021-01-25.
[60] F. Furche, R. Ahlrichs, C. Hättig, W. Klopper, M. Sierka, F. Weigend, *WIREs Comput. Mol. Sci.* **2014**, *4*, 91 – 100.
[61] R. Ahlrichs, M. Bär, M. Häser, H. Horn, C. Kölmel, *Chem. Phys. Lett.* **1989**, *162*, 165 – 169.
[62] R. Łazarski, A. M. Burow, M. Sierka, *J. Chem. Theory Comput.* **2015**, *11*, 3029 – 3041.
[63] R. Łazarski, A. M. Burow, L. Grajciar, M. Sierka, *J. Comput. Chem.* **2016**, *37*, 2518 – 2526.
[64] A. M. Burow, M. Sierka, *J. Chem. Theory Comput.* **2011**, *7*, 3097 – 3104.
[65] K. A. Peterson, D. Figgen, E. Goll, H. Stoll, M. Dolg, *J. Chem. Phys.* **2003**, *119*, 11113 – 11123.
[66] M. Brehm, B. Kirchner, *J. Chem. Inf. Model.* **2011**, *51*, 2007 – 2023.

Manuscript received: February 22, 2021
Version of record online: May 7, 2021

